

# Using dynamic modelling to simulate the distribution of rockglaciers

Regula Frauenfelder <sup>a,\*</sup>, Bernhard Schneider <sup>b</sup>, Andreas Kääh <sup>a</sup>

<sup>a</sup> *Department of Geography, University of Zurich, 8057 Zurich, Switzerland*

<sup>b</sup> *Department of Geosciences, University of Basel, 4056 Basel, Switzerland*

Received 17 September 2005; accepted 19 December 2006

Available online 5 May 2007

---

## Abstract

Rockglaciers — permafrost creep features on mountain slopes — are common landforms in high mountain areas. The present contribution reports about the exploration of a dynamic modelling approach using cellular automata to assess their regional distribution patterns. The designed prototype model allows the numerical simulation of the spatial and temporal occurrence of talus-derived rockglaciers in the Upper Engadine (eastern Swiss Alps) during the Holocene. The dynamic model considers processes in the spatial and temporal domain and accounts for both external and internal processes, implemented by means of six modules (A to G). The external processes are: (A) rock-debris accumulation, (B) hydrology, (C) climate, (D) glacier extent. The internal processes are: (E) creep initiation, (F) advance rate, (G) creep termination. Comparison between field evidence and modelling results shows that the dynamic model enables the simulation of spatio-temporal creep processes on a regional scale, but that the model is highly dependent on the accurate modelling of the relevant (input) parameters. These deficiencies have been recognized and analyzed, and it is planned that future research activities will address these issues.

© 2007 Elsevier B.V. All rights reserved.

**Keywords:** Creeping mountain permafrost; Dynamic modelling; Cellular automata; Swiss Alps; Holocene landscape history

---

## 1. Thematic background and aim

Rockglaciers are periglacial debris accumulations produced, deposited, and deformed over time scales of centuries to millenia. They are efficient transport systems of rock-debris in the periglacial alpine environment. Rockglaciers originate from talus ('talus-derived' rockglaciers, see Fig. 1) and/or glacier-transported debris.

Talus-derived rockglaciers are located at the foot of headwalls with a high supply of debris and represent a process chain linking frost weathering and rockfall (low

magnitude/high frequency events), and rock slides and debris flows (high-magnitude/low frequency events) from headwalls with debris displacement by permafrost creep. In general, the occurrence of these landforms is influenced primarily by climatic, topographic and geological preconditions.

Measured ice contents in active rockglaciers are in the order of 50 and 90% (e.g. Haeberli et al., 1998; Konrad et al., 1999; Vonder Mühll et al., 2001; Arenson, 2002), i.e. the ice content is significantly larger than the pore volume. This implies that active rockglaciers are super-saturated in ice, including massive ice lenses. Ice-supersaturated debris bodies deform under the influence of gravitational stress. This process leads to the formation of rockglacier landforms over time. Two main thermo-mechanical differences to the deformation of

---

\* Corresponding author. Department of Geosciences, University of Oslo, P.O. Box 1042 Blindern, 0316 Oslo, Norway.

E-mail address: [regula.frauenfelder@geo.uio.no](mailto:regula.frauenfelder@geo.uio.no) (R. Frauenfelder).

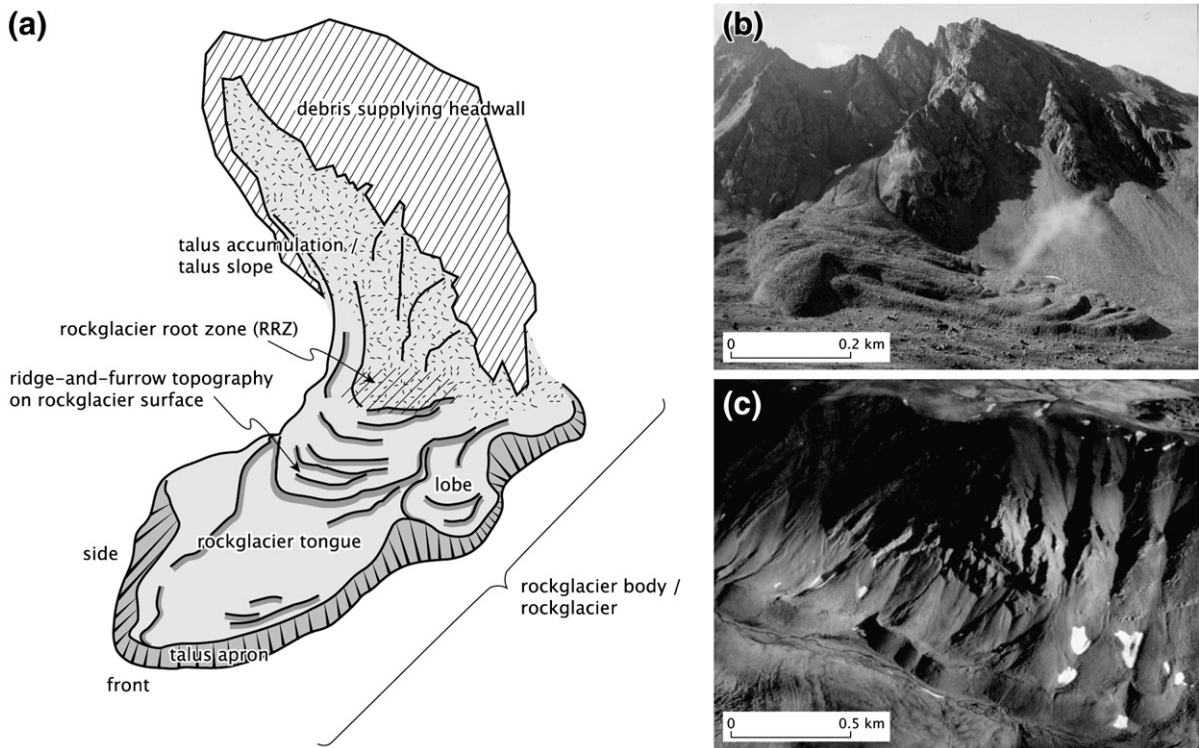


Fig. 1. (a) Schematic plot of a talus-derived rockglacier, (b, c) two examples of active talus-derived rockglaciers: (b) Muragl rockglacier in the Upper Engadine, Eastern Swiss Alps (photograph by R. Frauenfelder), (c) rockglaciers at Nordenskiöldkysten, Svalbard Archipelago (photograph by A. Kääh).

glacier ice should be noted: (1) the ice in rockglaciers is colder than 0 °C throughout the year, i.e. it is permanently frozen (= permafrost), and (2) the creeping body consists of a mixture of ice and debris. Although rockglacier matrices differ, therefore, significantly from glacier ice, first model attempts and sensitivity studies (e.g. Olyphant, 1983; Olyphant, 1987; Whalley and Martin, 1992; Arenson, 2002; Leysinger Vieli, 2004) suggest that the deformation of rockglacier bodies can be approximated quite well using Glen's flow law, though with rate factors very different to pure glacier ice.

Numerous inventory studies about rockglaciers yielded valuable information about their characteristics such as form, geology, location, etc. In addition, detailed studies on individual rockglaciers helped to build up a profound knowledge basis about these landforms. However, a comprehensive understanding of intra-regional variability of rockglacier occurrence is still lacking. The aim of the present study is, therefore, to help evaluate and increase knowledge about dynamics and distribution patterns of rockglaciers by means of dynamic modelling (cf. Bras et al., 2003, for an in-depth discussion of mathematical modelling in geomorphology).

## 2. Methodical background

Dynamic modelling builds upon static modelling by incorporating the time component (e.g. Van Deursen, 1995; Wesseling et al., 1996; Karssenbergh, 2002). A dynamic model describes, thus, how a parameter system can transform from one qualitative state into another, where each qualitative state is described by a static model. The dynamic spatio-temporal behaviour of the system is modelled as an interaction between spatial and temporal processes. The word 'spatial' refers to the geographic domain which the model represents (i.e. the two- or three-dimensional space), while 'temporal' refers to simulated changes through time by using rules of cause and effect (Lundell, 1996).

The presented dynamic model (cf. Section 4) is based on the approach of cellular automata (Von Neumann, 1966). Cellular automata are dynamical systems in which space and time are discrete. A cellular automaton consists of a regular grid of cells, each of which can be in one of a finite number of  $k$  possible states, updated synchronously in discrete time steps according to a local, identical interaction rule. The state of a cell is determined by the

previous states of a surrounding neighbourhood of cells (Sipper, 1997).

The model allows the numerical simulation of the spatial and temporal evolution of rockglacier occurrence and was tested for the region of the Upper Engadine. The time scale considered encompasses the entire Holocene (i.e. the last 10,000 years) but can also be extended into the future or further back into the past (i.e. the Lateglacial).

### 3. 'Pre-Holocene' topography of the Field area

Technically, each digital elevation model (DEM) with a resolution sufficient to adequately represent rockglacier features — spatial resolution denser or equal to ca. 30 m — can be used as an input for the model (cf. Section 4). For the testing of the prototype model, a DEM with 25 m cell size from *swisstopo* (the former Swiss Federal Office of Topography) was used. This so-called DEM25 is generated from the height information of the national 1:25,000 maps through vectorization of contour lines and lake contours, digitizing of the spot heights, and subsequent interpolation of a DEM with 25 m raster width from these data. Comparisons with photogrammetrically determined control points have shown that the average accuracy reaches approximately 3 m in the Alps (Hurni, 1995).

This DEM portrays the topographic surface including the rockglaciers. Therefore, the rockglaciers have to be extracted from the DEM before modelling. With a few exceptions, the bedrock topography below the rockglaciers in the study area is not known. In order to obtain a 'pre-Holocene' DEM devoid of rockglaciers, the existing DEM was transformed into a point layer, where each original grid cell is represented by one point. For rockglaciers with known bedrock topography (data from Vonder Mühll and Holub, 1992; Vonder Mühll, 1993; Arenson et al., 2002) the height of the points were set to the bedrock heights reported. For rockglaciers with unknown bedrock topography, the points were set to values equal to the values of the surrounding talus slopes. Finally, a new surface topography was interpolated from this altered point layer. The resulting DEM was then used for the modelling. Possible problems arising from this procedure are discussed in Section 6.

### 4. Structure of the dynamic model

The dynamic model considers processes in the spatial and temporal domain and accounts for both external and internal processes (see Fig. 2), implemented by means of six modules (A to G).

The external processes considered are:

- (A) rock-debris accumulation,
- (B) hydrology,
- (C) climate,
- (D) glacier extent.

The internal processes are:

- (E) creep initiation ('trigger'),
- (F) advance rate,
- (G) creep termination.

The model has been implemented as a stand-alone program. Crucial parameters, e.g. flow law parameters, climate parameters, and glacier extent history, are entered in editable spreadsheets before a model run. This allows for easy testing of the model. The program is written in C++, while the input grids are generated in Arc/Info.

#### 4.1. External processes

##### 4.1.1. Module A: rock-debris accumulation

In this module, the following four questions are resolved:

- (i) Where are the contributing rock walls?
  - (ii) Where are the debris accumulation areas and what is their extent?
  - (iii) How thick are the debris accumulations?
  - (iv) Which postglacial debris supply rates can be considered reasonable?
- (i) A simple method for identifying rockfall source areas in DEMs is the defining of thresholds for mean slope gradients (Dorren, 2003). In the present test area, values above 37° showed the best agreement with rock walls as mapped in the 1:25,000 Swiss Topographical Maps of the area. For a study area in the Valais Alps, M. Zemp (personal communication, 2002) found that best results are achieved when modelling rock walls as areas steeper than 34°. Van Dijke and van Westen (1990) defined potential rockfall source cells by a mean slope gradient greater than 60° (this implies that only very steep rock walls are considered). The broad range of values found in the literature shows that the threshold values have to be parameterized in each study area individually. More complex identifications of rockfall source areas on the basis of a GIS could include: aspect, slope

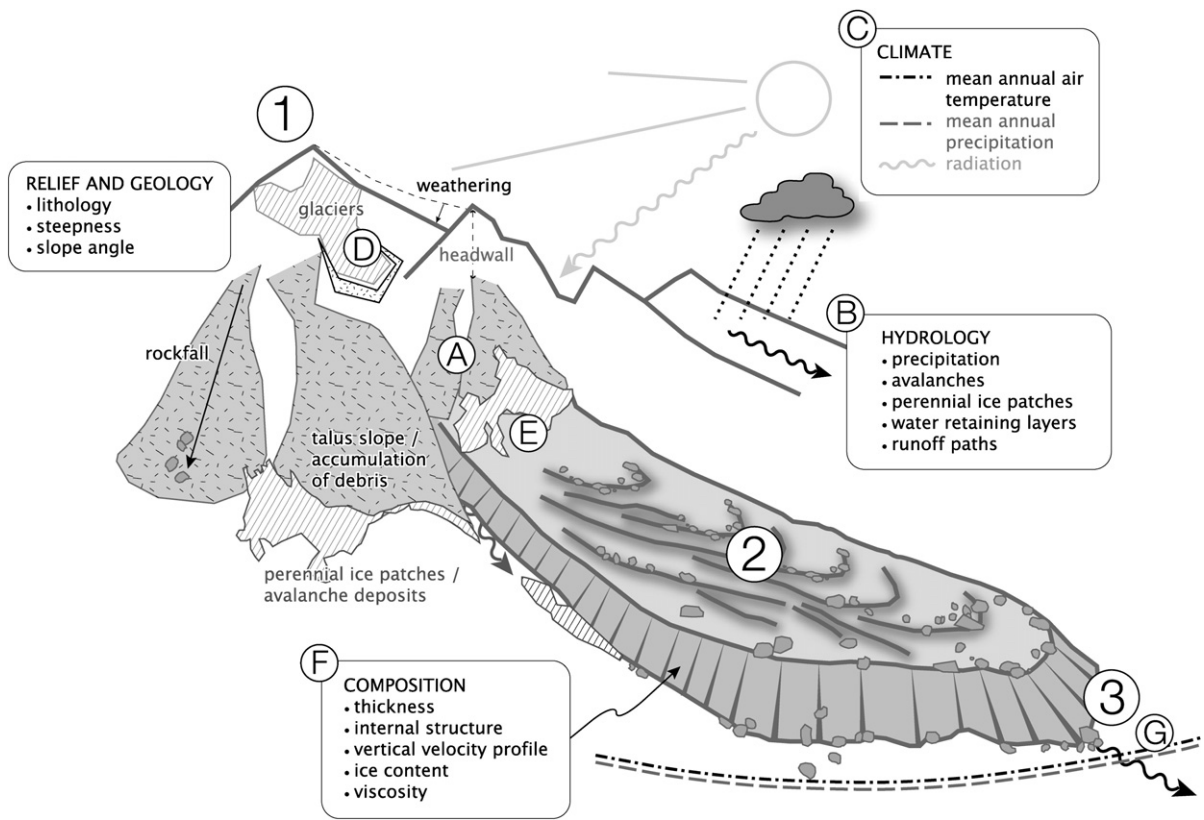


Fig. 2. Qualitative sketch of important boundary conditions for: ① the initiation (modules A–E), ② the growth (modules A–F), and ③ the inactivation/relictification (modules A, C, D, F, G) of a talus-derived rockglacier. See text for further explanations.

curvature, slope gradient, rock type and land cover (Dorren, 2003). A further crucial parameter for the production of debris is the geology. Debris production is highest in strongly deformed and disintegrated rocks. The deformation style of rocks is, in turn, dependent of geomechanical properties (jointing, faulting, bedding, etc.), geotechnical properties (hardness, stability, etc.), and hydrological properties (pore water, etc.). Although not addressed in the presented prototype model, these parameters would have to be considered in a more advanced version of the model.

- (ii) Rockfall is defined as “free falling blocks of different sizes (smaller than  $5 \text{ m}^3$ ) that detach from a cliff or a steep rock wall, show no interactions among each other, and follow an independent propagation mode” (Hübl et al., 2002). The extent of the debris accumulation areas is calculated using a programme by Brändli (2001) which is based on the so-called ‘overall-slope’ or ‘reach-angle’ approach, also known as ‘Fahrböschung’ (Heim, 1932). Rocks are simulated to fall from the contributing headwalls, i.e. the debris sources,

and to follow the path of steepest descent. The movement of falling rocks is assumed to stop when the slope of the straight line connecting the current position of the rock with its origin reaches  $31^\circ$ , which is an empirically derived value (Gerber, 1994). All cells that a rock passes during its fall are marked as ‘rock accumulation areas’. Finally, areas of contributing headwalls are excluded from these ‘rock accumulation areas’.

- (iii) The thickness of talus accumulation is variable and depends mainly on the debris production of the headwall (i.e. on headwall height, lithology, geology, permafrost absence/presence, climate, etc.) and the original relief of the slope beneath the headwall. Based on the investigation of a small sample of comparably large talus accumulations, some authors give typical thicknesses of alpine talus accumulations as 30 to 50 m. They describe the course of the slope bedrock as ‘often quasi parallel to the surface slope until close to the foot of the headwall’ (VAW, 1992a,b). Because of the lack of accessible information about the parameterization of talus thickness, a rough approximation of the



debris thickness is used: for each debris accumulation area the length between its highest and its lowest point is calculated. Then the maximum thickness of the layer is approximated as 10% of this accumulation area length, with the maximum in the middle of the distance and a parabolic decrease in thickness towards the edges of the accumulation area (Fig. 3). Although this approach neglects factors important on a local scale (e.g. bedrock topography, valley fill, etc.) it seems suitable for modelling on a regional scale. A comparison between modelling results and values reported by C. Hauck (personal communication, 2003) and in the VAW report cited above, shows that the method results in reasonable first-order approximations of talus thicknesses in the Eastern Swiss Alps.

- (iv) Rates of rock wall retreat have been evaluated by different methods. For the most part, the computations are based on the volume of sediments at the base of a rock wall, a procedure which yields long-term average rock wall retreat rates (Barsch, 1977; Ballantyne and Kirkbride, 1987; Hoffmann and Schrott, 2002). A few of the values are based on direct observations (e.g. Rapp, 1960; Matsuoka, 1990; Prick, 2003). For the Alps, estimated values of postglacial denudation rates are in the

order of  $0.1$  to  $>3 \text{ mm a}^{-1}$  (Poser, 1954; Barsch, 1977; Hoffmann and Schrott, 2002). Spatial heterogeneity of weathering rates and, hence, debris supply rates (caused by different geomechanical and geotechnical properties of the headwall) is known to be an important factor in many cases (e.g. Matsuoka and Ikeda, 2001). However, due to the initial stage of this model development and given the regional coverage aimed at, it was not possible to consider such heterogeneities.

The prototype model presented here operates with a ‘debris supply module’ that allows debris supply into the cells which already contain debris at the start of a model run, i.e. into the initial debris distribution cells, or in other words, into cells representing talus slopes. Different ‘supply’ procedures were tested, ranging from the supply of a given amount of debris per year to complete refilling of a cell if its debris content decreases to a value lower than the initial value.

#### 4.1.2. Module B: hydrology

The influence of water on the formation of rock-glaciers has been scarcely investigated to date. As a result, the prototype model has been simplified as follows: (1) the lithological preconditions relative to

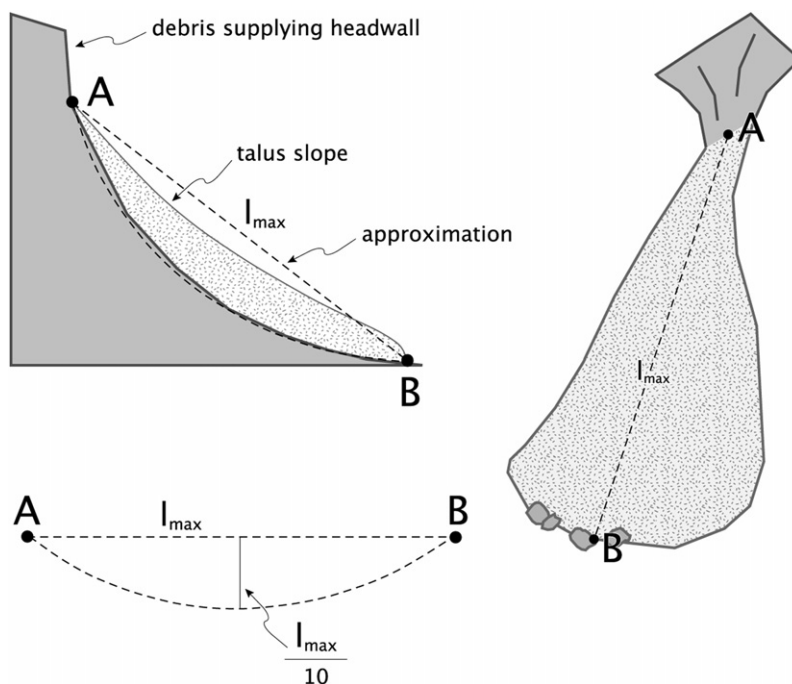


Fig. 3. Parabolic approximation of talus thickness (schematic, not to scale): for each talus the length between its highest and its lowest point is calculated. Then the maximum thickness of the talus is approximated as 10% of the measured talus length, with the maximum in the middle of the distance and a parabolic decrease in thickness towards the edges of the talus.

water storage capabilities are assumed to be spatially homogenous; (2) the topographical preconditions for water storage (concavity, convexity, etc.) are approximated with the wetness index of the terrain (e.g. [Beven and Kirkby, 1979](#); [Moore et al., 1990](#)), which is calculated by means of the drainage routine described by ([Skaug, 2000](#)). His algorithm calculates runoff from a raster-based terrain model and allows — in contrast to the most frequently used runoff algorithms — directing outflow of one raster-cell into two or more adjacent lower cells (“divergent flow”); (3) any possibly existing differences in the snow depletion history are neglected.

#### 4.1.3. Module C: climate

Climate (i.e. temperature, precipitation, radiation) has a significant influence on the thermal state of the ground (e.g. [Stocker-Mittaz et al., 2002](#)). Theoretically, this range of influences could be accounted for by the combination of three modules: one for temperature (including isotherms, the regional temperature gradient, a climate factor to cool/warm the climate, etc.), one for radiation (including radiation thresholds for the formation of frozen ground, cloud cover intensities during different phases of the Holocene, etc.), and one for precipitation (including isohyets, regional precipitation gradient, information about precipitation changes during the Holocene, etc.). In the present prototype, temperature and radiation influences are approximated by the inclusion of permafrost distributions at different points in time, modelled with the PERMAP model ([Hoelzle, 1994, 1996](#)). This permafrost model incorporates the influences of the mean annual air temperature (MAAT) and the potential direct solar radiation on the thermal state of the ground. The permafrost distribution as modelled with this program is, hence, considered as a proxy of the thermal and radiation-induced influences of climate.

Two main permafrost extents have been modelled for initial tests:

- (1) Present conditions: extent under the current temperature realm
- (2) ‘Little Ice Age’ conditions: extent with a MAAT = 1 °C lower than at present

The period of validity for each stage is inferred from glacier and climate reconstructions for the Holocene, mainly from [Maisch et al. \(2000\)](#), [Roberts \(2000\)](#), and [Labeyrie et al. \(2003\)](#). In this initial stage of the model, precipitation is assumed to be spatially and temporally homogenous. Although Alpine precipitation can vary significantly at local scale, spatial homogeneity on a

regional scale seems to be justified for the area in question by the regional precipitation interpolation of [Schwarb et al. \(2000\)](#). The assumption of a temporal homogeneity, however, is certainly a subject of debate.

#### 4.1.4. Module D: glacier extent

Due to varying climate conditions during the Holocene, glacier extents changed extensively, oscillating at various times between the maximum extent reached during the ‘Little Ice Age’ (LIA) and the minimum extent reached probably during the prime of the Holocene temperature optimum (8000–5000 y BP).

Two different glacier extents are integrated into the model:

- (1) Glacier extent from 1999 ([Paul, 2003](#))
- (2) Glacier extent around 1850, the Alpine maximum extent of the LIA ([Maisch, 1992](#))

As in Module C, periods of validity for the different glacier extents are determined from studies by [Maisch et al. \(2000\)](#), [Roberts \(2000\)](#), and [Labeyrie et al. \(2003\)](#), and in addition, from reports about minimum glacier extents during the Holocene, e.g. from [Haeberli et al. \(2004\)](#), [Holzhauser \(1995\)](#), and [Joerin and Schlüchter \(2005\)](#).

### 4.2. Internal processes

#### 4.2.1. Module E: creep initiation (‘trigger’)

This module determines whether creep is initiated or not. Creeping is described as a flow process which is affected by parameters such as shear stress and viscosity differences at material boundaries. When sliding at the bed is neglected (as suggested for rockglaciers by [Haeberli, 1985](#)), the largest amount of the movement can be attributed to the plastic deformation of the ice-content of the ice-debris matrix. In rockglacier science, this deformation has been described most often until present by using Glen’s glacier flow law for pure ice ([Glen, 1955](#); [Paterson, 1994](#); cf. Section 1):

$$\dot{\epsilon} = A\tau^n \quad (1)$$

where  $\dot{\epsilon}$  is the strain rate,  $\tau$  the shear stress,  $A$  the flow or rate factor and  $n$  a dimensionless power law exponent.  $A$  depends on the ice temperature (warm ice=‘soft’, cold ice=‘brittle’), the unfrozen water content, the size of the ice crystals and the amount of fine-grained sediment in the ice.  $n$  depends upon a variety of conditions, for example, overload. For large, thick glaciers  $n$  is usually set at 3, for the considerably smaller, thinner rockglaciers,  $n$  is set at 1

(Wagner, 1996). Both  $A$  and  $n$  are empirically determined and various values for glaciers can be found in the literature (e.g. Paterson, 1994).

Glen's glacier flow law states that deformation of the ice starts if the thickness of the ice exceeds a critical value, or in other words, when a critical threshold for the basal shear stress  $\tau$  is surpassed. The basal shear stress  $\tau$  is described as:

$$\tau = \rho g h \sin \alpha \quad (2)$$

with  $\rho$  the density of the rock–ice mixture,  $g$  the acceleration due to gravity ( $9.81 \text{ ms}^{-2}$ ),  $h$  the thickness of the frozen debris layer, and  $\alpha$  the surface slope averaged over a length of  $5h$  along the path of steepest descent. Values for  $\rho$  are taken from borehole measurements as reported, for example, by Barsch et al. (1979), Wagner (1992), Vonder Mühll (1993), and Arenson (2002) and are in the order of  $1.5\text{--}1.8 \text{ g cm}^{-3}$ .

A rockglacier matrix has to be supersaturated in ice to allow creep deformation. Therefore, the volumetric increase of the talus accumulation caused by this ice content, has to be considered in a model. Exact values for this volumetric increase are not known. Based on observations from drilling, it can be assumed that the overall ice content in supersaturated frozen rockglacier sediments is higher than the porosity of comparable non-frozen sediments by a factor of two to three (e.g. Barsch et al., 1979; Haeberli, 1985; Konrad and Humphrey, 2000; Arenson, 2002).

Creep initiation is tested for by analyzing whether the topographic settings lead to a shear stress within the creeping matrix that is large enough to initiate cumulative deformation. The minimal shear stress is taken as  $\tau=50 \text{ kPa}$ , an empirical value derived from borehole measurements (Wagner, 1996). When this value is exceeded, a cell is considered as starting to creep. It has to be noted that the time lags after which rockglaciers react to changes in climate and/or debris supply rates (cf. Olyphant, 1987) are not accounted for in the present version of the model.

#### 4.2.2. Module F: advance rate

If creeping is possible, the movement of the rockglacier is calculated. The surface velocity is calculated according to Glen's flow law for glaciers:

$$v_s - v(z) = \frac{2A}{n+1} (F\rho g \sin \alpha)^n (h-z)^{n+1} \quad (3)$$

$$v_s - v_b = \frac{2A}{n+1} (F\rho g \sin \alpha)^n h^{n+1} \quad (4)$$

where  $v_b$  is the velocity at the base,  $v$  is the velocity at depth  $(h-z)$ ,  $F$  is a shape factor, and all other parameters are the same as in Eqs. (1) and (2).  $F$  is dependent on the bed topography and considers the friction at the valley flanks (Paterson, 1994). In the present model, values for  $A$  were taken from borehole measurements at Murtèl rockglacier as determined by Wagner (1996). In addition, a new value for  $A$  was determined by reproducing empirically measured flow velocities of three Alpine rockglaciers (Frauenfelder et al., 2005) using  $n=1$  and  $F=0.75$ . This value for  $A$  equals  $1.2 \cdot 10^{-12} \text{ s}^{-1} \text{ kPa}^{-n}$ , a value in the same order of magnitude as the values given for the ice-rich layer (without the soft-deforming layer) at Murtèl when  $n$  equals 1 or 1.1, respectively (Wagner, 1996). Both Wagner's values and the value for  $A$  determined here are notably higher than the values calculated for glaciers. Wagner (1996) found that with equal shear stress ( $\tau=40 \text{ kPa}$ ) and temperature, the strain rate  $\dot{\epsilon}$  of the ice in the rockglacier Murtèl is slightly higher than for glacier ice.

The average velocity  $\bar{v}$  at which a rockglacier creeps can be considerably smaller than the maximal velocity which is found at its surface  $v_s$  (see Fig. 4). Integration of Eq. (3) gives  $\bar{v}$ , the velocity averaged over the total thickness of the rockglacier body:

$$\bar{v} = \frac{1}{h} \int_0^h v(z) dz = \frac{2A}{n+2} (F\rho g \sin \alpha)^n h^{n+1} \quad (5)$$

The advance rate  $v_{\text{adv.}}$ , however, is not only a function of the form of the velocity profile (see below), but also of the melting and re-freezing of ice/water within the advancing material. The ice in the ice-debris matrix, especially in the fine-grained layers at the rockglacier front, is not shielded against temperature and radiation as well as it is within the coarse blocky surface layer. As a result, heat can penetrate more efficiently into the matrix and cause (considerable) ice melting. This leads to a further reduction of the advance rate of the rockglacier. To account for this, a correction factor  $C_{\text{melt}}$  is included. The advance rate  $v_{\text{adv.}}$  subsequently used in the model is then calculated as:

$$v_{\text{adv.}} = C_{\text{melt}} \bar{v} = C_{\text{melt}} \left( \frac{2A}{n+2} (F\rho g \sin \alpha)^n h^{n+1} \right) \quad (6)$$

Precise values for  $C_{\text{melt}}$  are scarce. Kääb (2005) derived empirical values accounting for both the velocity decrease with depth and reduction of the advance rate due to ice melt from field measurements. These values range from 0.1 to 0.5, depending on the ice content of the rockglacier. With  $n=1$  and  $\bar{v}=2/3 v_s$  (Paterson, 1994)

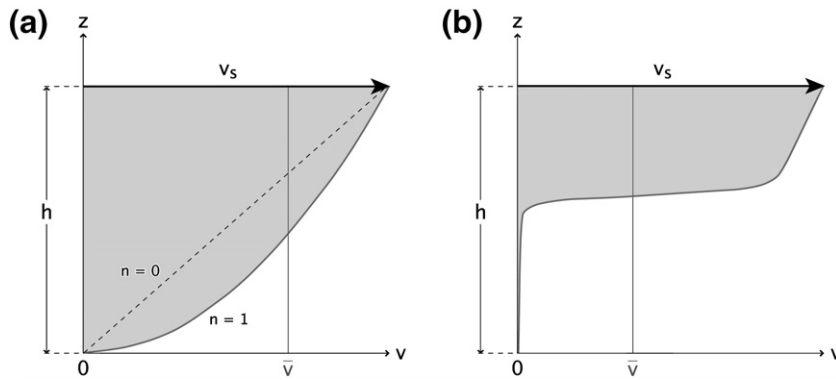


Fig. 4. Sketches of selected velocity profiles of a creeping rockglacier mass, with  $z$ =depth,  $h$ =thickness of creeping mass,  $v_s$ =maximal surface velocity,  $\bar{v}$ =average velocity. (a) Velocity profiles for  $n=0$  and  $n=1$ , respectively, (b) velocity profile as deducible from borehole measurements. The in-situ measurements on four Alpine rockglaciers suggest that they are all characterized by a (comparably thin) shear zone with deformations of 50 to 97% of the total surface deformation (Arenson et al., 2002). As the depth of these shear zones seems to vary for different rockglaciers and modelling of their depths has, thus far, not been performed, this phenomenon is not considered in the model presented here.

values for  $C_{\text{melt}}$  result in 0.15–0.75. The advance rate  $v_{\text{adv}}$ , multiplied by the time step  $\Delta t$  yields the distance the rockglacier front moves forward during  $\Delta t$ .

#### 4.2.3. Module G: creep termination

Several conditions can lead to the halt of a rockglacier, subsequently causing either its climatic or dynamic inactivity:

- (a) Climatic inactivity due to movement of the rockglacier into non-permafrost areas, either actively by creeping or, passively due to a rise in the permafrost limit.
- (b) Dynamic inactivity caused by:
  - topographic blockage (e.g. shallow or increasing slope), and/or
  - reduction in debris supply, and/or
  - decreasing ice incorporation.

In both cases the rockglacier's inactivation and, subsequently its relictification, is governed by the high

thermal inertia of the system. In the model, climatic inactivity (a) is automatically induced when the lowest cell of a rockglacier reaches the permafrost limit. Dynamic activity (b) is accounted for by Eq. (2): if the slope and/or the debris thickness fall below a threshold necessary to keep up the required shear stress, the velocity approximates zero.

#### 4.3. Emphasis

The emphasis of the model is on the creep of the debris–ice mass, i.e. the transport of volume from one cell to the next. The modelling includes control of creep initiation and tracking of changes in thickness of the debris–ice mass. Fig. 5 shows the modelling scheme: situation (a) shows two cells, an upper one, holding a volume of debris–ice mass, and a lower one, devoid of mass. The mass is creeping with  $\bar{v}$ , the velocity averaged over the total thickness of the rockglacier body, i.e. the accumulated thickness; (b) during a time step  $\Delta t$ , the mass is transported forward over the distance  $d$ ; (c) the

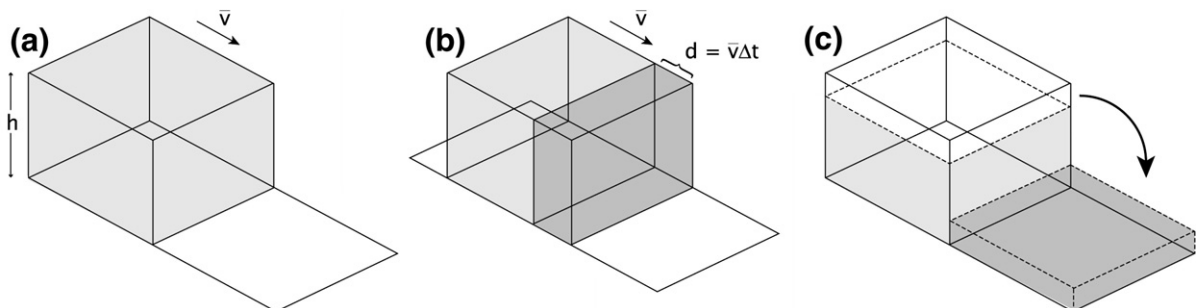


Fig. 5. Schematic plot of the modelling scheme, explaining how volume is transported from one cell to the next. See text for further explanations.



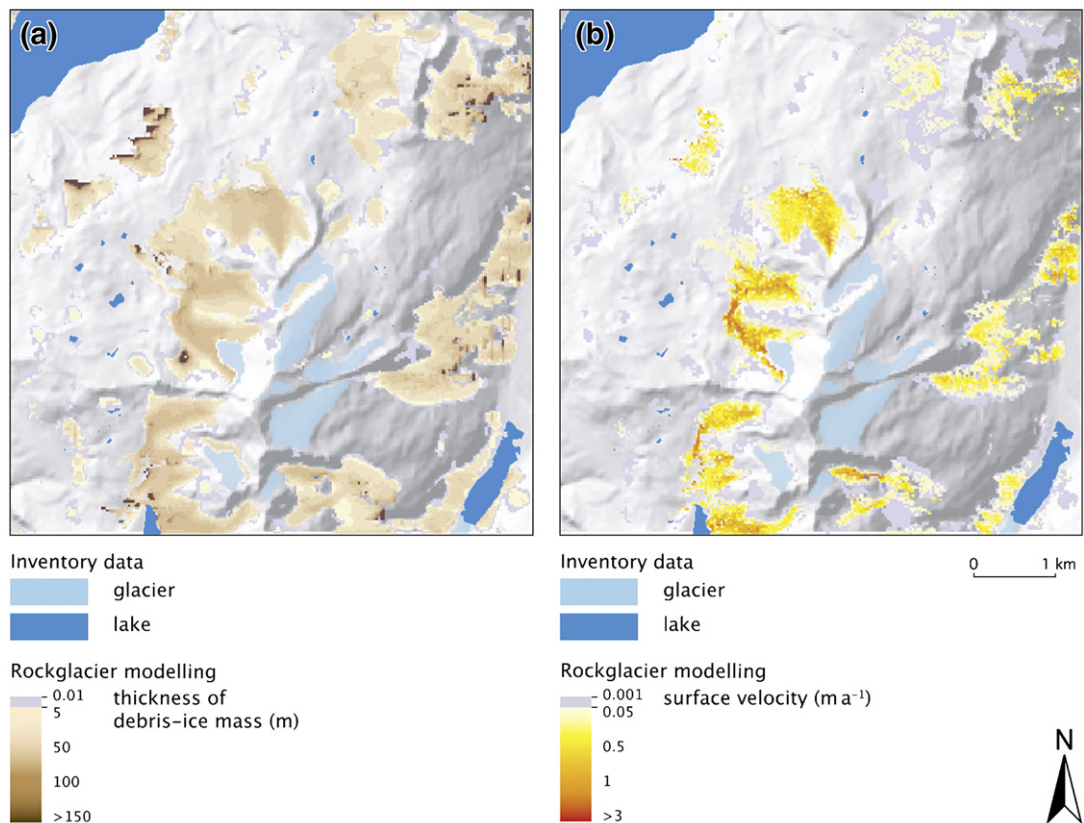


Fig. 6. Results I: rockglacier distribution modelling for a test area in the Corvatsch–Furtschellas region, Upper Engadine, Switzerland. Situation after 10,000 years: (a) thickness distribution, (b) velocity distribution. Glacier extent corresponds to the extent in 1999 and was extracted from satellite images by Paul (2003). Background: DEM25 © 2004 swisstopo (BA045979). Model parameters:  $n=1$ ,  $A=1.2 \cdot 10^{-12} \text{ s}^{-1} \text{ kPa}^{-n}$ .

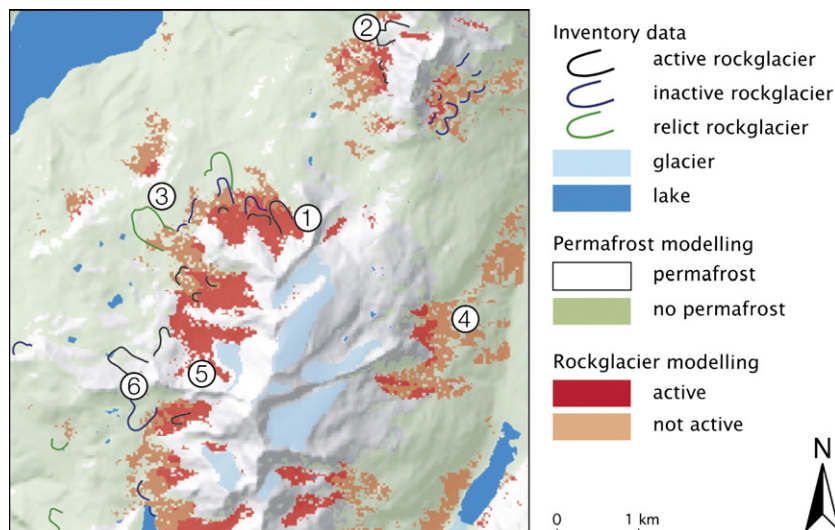


Fig. 7. Results II: rockglacier distribution modelling for a test area in the Corvatsch–Furtschellas region, Upper Engadine, Switzerland. Red and pink zones represent 'modelled rockglaciers' and are areas where thickness of the debris–ice mass is  $\geq 5 \text{ m}$  and velocities are  $>0.05 \text{ m a}^{-1}$  (see Fig. 6). Red zones represent active rockglaciers, i.e. rockglaciers presently affected by permafrost, pink zones represent rockglaciers that have been active during some period of the model run but are not under permafrost conditions anymore. Glacier extent as in Fig. 6, rockglacier distribution as inventoried by Hoelzle (unpublished; 1998). Background: DEM25 © 2004 swisstopo (BA045979). Model parameters as in Fig. 6.

advanced mass is interpreted as an overflow from cell to cell: the upper cell loses a corresponding amount of its thickness, while the lower cell is filled evenly with the analogous amount. In the initial debris cells (but exclusively in those) the ‘debris supply module’ allows a refilling of the discharged mass volume if the thickness in these cells becomes less than their initial thickness (i.e. if they discharge more mass than they receive from their upslope cells). This enables the inclusion of (continuous) debris supply during a model run. After a complete model run, two output grids are written: the ‘thickness distribution’ and the ‘velocity distribution’ of the creeping debris–ice mass.

The model is evaluated by subsequently introducing alterations into the debris transport chain: (a) rockglacier initiation with and without a trigger for debris creep, (b) non-stochastic and probabilistic random flow direction for debris, (c) velocity decrease (accounting for the fact that surface velocity is not equal to advance rate), (d) thermal inertia of the debris–ice matrix (allowing rockglaciers to creep several tens of metres out of the permafrost zone).

## 5. Initial results and discussion

Fig. 6 shows the result of a model run for 10,000 years for the Corvatsch–Furtschellas test region, Upper Engadine, Switzerland. For a model run with  $n=1$ ,  $A=1.2 \cdot 10^{-12} \text{ s}^{-1} \text{ kPa}^{-n}$ , modelled debris thicknesses range in the order of a few centimetres to over 100 m. Modelled velocities are in the order of centimetres to metres per year. Compared to field evidence, debris thicknesses of up to ca. 100 m and velocities below  $1.5 \text{ m a}^{-1}$  are seen as reasonable values for the area concerned (cf. Vonder Mühll, 1993 for debris thicknesses of active rockglaciers, and e.g. Kääb and Vollmer, 2000; Roer et al., 2005 for velocity measurements). Higher debris thicknesses (exceeding 100 m thickness) and higher velocities (over  $2 \text{ m a}^{-1}$ ) are reached at the edge of the model perimeter (e.g. right border of the test area) and in some local small-scale depressions. These are undesired side-effects of the modelling caused by the fact that debris cannot flow out of the model perimeter or further onto a flat plane and is, therefore, dammed up, which subsequently leads to increasing debris thickness and rising flow velocities.

The amount of debris supplied to the initial ‘talus’ cells during the aforementioned model run corresponds to roughly  $3\text{--}4 \text{ mm a}^{-1}$  vertical accumulation. These values are in the same order as rock wall retreat rates estimated by Barsch (1977), but considerably higher than those found, for example, by Hoffmann and Schrott

(2002). Two reasons might explain the comparably high values attained during the modelling: (a) rockfall is often highest along faults and fault zones, and most talus cones are developed at the foot of such zones (cf. Fig. 1). In addition, rockfall is often channelled in gullies and along natural topographic breaklines. Altogether, this leads to concentrated debris accumulation on the talus slopes. (b) As mentioned, ice content by volume in active talus-derived rockglaciers averages between 50 and 90% (e.g. Haeblerli et al., 1998; Vonder Mühll et al., 2001; Arenson, 2002). Setting these values against the modelled numbers, reduces modelled debris supply rates to  $0.3\text{--}2 \text{ mm a}^{-1}$ .

The modelling results are regarded as representations of rockglaciers where both debris thickness and velocity lie over user-defined thresholds. Characteristic mean active layer thicknesses in the study area are around 3 to 3.5 m in coarse blocky material and 4 to 5 m in rock walls (M. Hoelzle, personal communication, 2004). Velocities above  $0.05 \text{ m a}^{-1}$  are considered as indicators of ‘creep at a significant rate’. Hence, thicknesses greater than 5 m and velocities greater than  $0.05 \text{ m a}^{-1}$  were defined as thresholds for the identification of creeping debris and, consequently, cells above this threshold mapped as rockglaciers. Fig. 7 shows the rockglaciers that result when these thresholds are applied to the values visualized in Fig. 6.

Comparison between field evidence and modelling results yields the following (numbers refer to numerals in Fig. 7):

- 1 Most active and inactive talus-derived rockglaciers are reproduced accurately by the model, and the extents they exhibit in nature are also shown, approximately, in the model, although small deviations of course exist.
- 2 Certain active rockglaciers are not reproduced by the modelling. Careful consultation of the inventory data reveals that (at least) some of these rockglaciers developed from glacier-transported debris, and thus cannot be reproduced by a model that is based entirely on the processes involved in the development of talus-derived rockglaciers.
- 3 In a model run for 10,000 years, the modelled rockglacier fronts do not advance into regions where relict rockglaciers are found in the inventory. Based on temperature reconstructions (Frauenfelder and Kääb, 2000; Frauenfelder et al., 2001) and relative age dating on selected rockglaciers (Laustela et al., 2003; Frauenfelder et al., 2005), it can be assumed that relict rockglaciers in the area evolved as early as the Alpine Lateglacial. These findings seem to be supported by the model results

with ‘virtual rockglaciers’ not exceeding the extents of active (and some inactive) rockglaciers.

- 4/5 The areas modelled as being affected by creeping are considerably larger than the areas in which creep features have actually been observed in field investigations. Such ‘overestimations’ occur both in areas outside the present permafrost distribution (cf. 4), and within the current permafrost zone. Possible explanations for these deviations involve time, relations between debris supply rates and creep rates, thermal dependence of creep rates, hydrological preconditions, composition of the talus slopes (fine-grained, coarse-grained), etc. In certain cases (cf. 5), the overestimations are localized in glacier forefields that became deglaciated after the LIA. Here, the errors are based on the fact that the permafrost distribution used as an input variable for the model does not take into account the absence/discontinuity of permafrost in recently deglaciated areas.
- 6 Some talus-derived rockglaciers were not captured by the model due to ‘inaccuracies’ of the input DEM (i.e. too coarse resolution to capture detailed topography), which lead to a underestimation of the talus input calculation.

## 6. Main challenges

In general, the simulation of regional rockglacier distribution with the prototype model shows promising results. Nonetheless, the preliminary findings also reveal some major problems involved with the modelling approach applied. They have been recognized and analyzed and are summarized below. Future research activities should address these issues.

- Availability of rock-debris: the availability of rock-debris has been identified as a very important parameter. It is, however, very difficult to model. In the prototype model, uncertainty about the debris availability arises from three main sources: (a) the simplified identification of debris-producing headwalls, (b) the difficulty in estimating the thickness of rockfall accumulations, and (c) the uncertainty relating to postglacial debris supply rates.
  - (a) In the present version of the model, all slopes steeper than 37° are considered as debris-producing headwalls. Although feasible as a crude approximation, this simple approach is a source of large errors. For instance, differences in production rates due to different geological characteristics cannot be accounted for. A future version of the model should allow a better parameterization of debris-producing headwalls, including regional calibration. This would allow a better estimation of the debris input into the system.
  - (b) A number of approaches are available to estimate the extent of debris accumulations, for example, from air- or space-borne remote sensing (e.g. Bishop et al., 1999; Kieffer et al., 2000; Taschner and Ranzi, 2002; Paul, 2003). Literature on the estimation of debris accumulation thickness, in contrast, is generally sparse. Only few data are available from geophysical measurements on individual scree slopes (e.g. VAW, 1992a,b; Kneisel et al., 2000; Delaloye et al., 2001; Gude et al., 2003; Hoffmann and Schrott, 2003). The talus thicknesses reported there generally agree with the values modelled here. Still, the applied estimation of the talus thickness is certainly a critical one.
  - (c) As mentioned before, great uncertainty exists about the amount of postglacial denudation in periglacial areas and, thus, the spatio-temporal characteristics of debris input into the model. On the other hand, the model presented here allows sensitivity studies to be performed in such a way that theoretical concepts of the spatio-temporal behaviour of debris supply can be tested with reference to their effect on modelled rockglacier distribution.
- Mass transport approach: A drawback of this approach is that the real advance of the rockglacier fronts is not modelled. The decrease of the advance rate due to frontal ice melt can, therefore, not be accounted for.
- Climatic limitation of rockglacier movement: in the present version of the model, the movement of a rockglacier stops as soon as the rockglacier’s front reaches the edge of the permafrost occurrence. This approach has two weaknesses: firstly, the calculation of the extent of the permafrost distribution is, to some extent, uncertain (e.g. Hoelzle, 1996; Imhof, 1996; Frauenfelder et al., 1998). Secondly, as mentioned before, the thermal inertia of ice and the rockglacier’s own microclimate (coarse blocky surface material, advective heat flow, turbulent fluxes, etc.) prevent its immediate melt when coming into unfavourable climate conditions.
- Digital elevation models depict present topographies: DEMs generated from maps or aerial photography portray the topographic surface including existing geomorphological forms such as,

for example, rockglaciers. The creeping occurs in layers below the visible surface. In most cases, neither the topography of these layers nor of the underlying bedrock is known. In the study area, the depth of both the shearing layers and the bedrock are known for a few rockglaciers only: for three rockglaciers from borehole inclinometer measurements (Vonder Mühll and Holub, 1992; Arenson et al., 2002), for one rockglacier from geoelectrical and seismic soundings (Vonder Mühll, 1993). The knowledge base for the extraction of rockglaciers from the DEM is, therefore, rather thin. Still, the rockglaciers had to be extracted in order to get a ‘Pre-Holocene’ topography. Interpolation of the topography before rockglacier initiation from the values of the surrounding neighbourhood, as effected in the present study (cf. above), is a possible but problematic solution to this problem: for the areas where rockglaciers are located in the ‘present-day’ DEM, interpolation produces height values comparable to the adjacent talus slopes where no creeping is observed today. In addition, presumably pre-existing concavities in the bedrock underneath the rockglaciers found today cannot be reproduced.

- Influence of the rate factor  $A$ : Various tests of the model yielded a high sensitivity of the velocity and, consequently, of the maximum debris thickness reached, to relatively small variations (in the range of several  $1.0 \cdot 10^{-12}$ ) of the rate factor  $A$ . This, in turn, greatly influences the rockglacier distribution present at the end of a model run. In the present model, all rockglaciers are modelled with one value for  $A$ , a simplification not given in nature. The inclusion of a spatio-temporally varying  $A$  would presumably lead to significantly improved modelling results, with several disagreements between modelling results and field evidence becoming explainable. Results from 2D numerical modelling (Kääb, 2005), laboratory testing (Arenson, 2002) and field evidence (Frauenfelder et al., 2003) have shown a clear temperature dependence of  $A$ . Therefore, the inclusion of a temperature-dependent spatial variation of  $A$  as an input parameter seems highly recommendable for a future version of the model.

## 7. Conclusions

As for every model, the dynamic model presented here is inherently based upon a number of assumptions. The model enables the simulation of spatio-temporal creep processes, but proves to be highly dependent on the accurate modelling of the relevant input parameters. The

quantification of the extent and thickness of rockfall accumulation and of postglacial debris supply rates, which are important input parameters for the model, is difficult. In addition, the inclusion of hydrological constraints is not easy because research on this subject is scant.

Despite the simplifications and deficiencies pointed out, the model provides a tool for further identification and evaluation of important parameters related to rockglacier initiation and growth, and also helps to illustrate the complexity of the ‘rockglacier’ phenomenon. In this respect, the modelling process promotes an increase in the knowledge of rockglacier distribution and also permits gaps in this knowledge to be highlighted and directions for crucial future research to be pointed out. Or using the words of C. Chatfield (1995): “All models are wrong, but some are useful”.

## Acknowledgements

The work of Regula Frauenfelder was financially supported by the ‘Stiftung zur Förderung der wissenschaftlichen Forschung an der Universität Zürich’. We are grateful for this support. Further thanks go to Wilfried Haeberli and Martin Hoelzle for the many important discussions, their comments greatly improved this contribution. We are also indebted to Frank Paul, who provided the digitized glacier data. Further thanks go to Othmar Wigger and his team, who tended the computer infrastructure 24 h a day, and solved (almost) all the hard- and software problems we managed to run into. Susan Braun–Clarke polished the English of an earlier manuscript on which this contribution is based. Last but not least we would like to thank two anonymous reviewers for their constructive comments.

## References

- Arenson, L.U., 2002. Unstable alpine permafrost: a potentially important natural hazard. Variations of Geotechnical behaviour with time and temperature. PhD Thesis, ETH Zurich. 271 pp.
- Arenson, L., Hoelzle, M., Springman, S., 2002. Borehole deformation measurements and internal structure of some rock glaciers in Switzerland. *Permafrost and Periglacial Processes* 13, 117–135.
- Ballantyne, C.K., Kirkbride, M.P., 1987. Rockfall activity in upland Britain during the Loch Lomond Stadial. *Geographical Journal* 153, 86–92.
- Barsch, D., 1977. Eine Abschätzung von Schuttproduktion und Schutttransport im Bereich aktiver Blockgletscher der Schweizer Alpen. *Zeitschrift für Geomorphologie* 28, 148–160.
- Barsch, D., Fierz, H., Haeberli, W., 1979. Shallow core drilling and borehole measurements in permafrost of an active rock glacier near the Grubengletscher, Wallis, Swiss Alps. *Arctic and Alpine Research* 11 (2), 215–228.
- Beven, K.J., Kirkby, M.J., 1979. A physically based, variable contribution area model of basin hydrology. *Hydrological Sciences* 24, 43–69.



- Bishop, M.P., Shroder, J.F.J., Hickman, B.L., 1999. SPOT Panchromatic imagery and neural networks for information extraction in a complex mountain environment. *Geocarto International* 14, 19–28.
- Bras, R.L., Tucker, G.E., Teles, V., 2003. Six myths about mathematical modeling in geomorphology. In: Wilcock, P., Iverson, R. (Eds.), *Prediction in Geomorphology*. American Geophysical Union, pp. 63–79.
- Chatfield, C., 1995. Model uncertainty, data mining and statistical inference. *Journal of the Royal Statistical Society. Series A, Statistics in Society* 158 (3), 419–466.
- Delaloye, R., Reynard, E., Lambiel, C., 2001. Pergélisol et construction de remontées mécaniques: l'exemple des Lapires (Mont-Gelé, Valais). *Frost in der Geotechnik — Le Gel en Géotechnique* 141, 103–113.
- Dorren, L.K.A., 2003. A review of rockfall mechanics and modelling approaches. *Progress in Physical Geography* 27, 69–87.
- Frauenfelder, R., Kääb, A., 2000. Towards a palaeoclimatic model of rock glacier formation in the Swiss Alps. *Annals of Glaciology* 31, 281–286.
- Frauenfelder, R., Allgöwer, B., Haeberli, W., Hoelzle, M., 1998. Permafrost investigations with GIS — a case study in the Fletschhorn area, Wallis, Swiss Alps. In: Lewkowicz, A.G., Allard, M. (Eds.), *7th International Conference on Permafrost. Proceedings. Collection Nordicana. Centre d'Etudes Nordiques, Université Laval, Yellowknife, Canada*, pp. 291–295.
- Frauenfelder, R., Haeberli, W., Hoelzle, M., Maisch, M., 2001. Using relict rockglaciers in GIS-based modelling to reconstruct Younger Dryas permafrost distribution patterns in the Err–Julier area, Swiss Alps. *Norwegian Journal of Geography* 55, 195–202.
- Frauenfelder, R., Haeberli, W., Hoelzle, M., 2003. Rockglacier occurrence and related terrain parameters in a study area of the Eastern Swiss Alps. In: Phillips, M., Springman, S., Arenson, L. (Eds.), *8th International Conference on Permafrost, Proceedings. Swets and Zeitlinger, Lisse, Zurich*, pp. 253–258.
- Frauenfelder, R., Laustela, M., Kääb, A., 2005. Relative age dating of Alpine rockglacier surfaces. *Zeitschrift für Geomorphologie N.F.* 49, 145–166.
- Gerber, W., 1994. Beurteilung des Prozesses Steinschlag. Schweiz. Forstl. Arbeitsgruppe Naturgefahren (FAN), Herbstkurs, 20.–22. Oktober 1994, Poschiavo. Kursunterlagen.
- Glen, J.W., 1955. The creep of polycrystalline ice. *Proceedings of the Royal Society of London. Series A* 228, 513–538.
- Gude, M., Hauck, C., Kneisel, C., Krause, S., Molenda, R., Ruzicka, V., Zacharda, M., 2003. Evaluation of permafrost conditions in non-alpine scree slopes in Central Europe by geophysical methods. EGS, 28th General Assembly, Nice, 08966 (CD-ROM).
- Haeberli, W., 1985. Creep of mountain permafrost. *Internal Structure and Flow of Alpine Rock Glaciers. Mitteilungen der VAW-ETH Zürich*, vol. 77, 142 pp.
- Haeberli, W., Hoelzle, M., Kääb, A., Keller, F., Vonder Mühll, D., Wagner, S., 1998. Ten years after drilling through the permafrost of the active rock glacier Murtèl, Eastern Swiss Alps: answered questions and new perspectives. In: Lewkowicz, A.G., Allard, M. (Eds.), *7th International Conference on Permafrost. Proceedings. Collection Nordicana. Centre d'Etudes Nordiques, Université Laval, Yellowknife, Canada*, pp. 403–410.
- Haeberli, W., Frauenfelder, R., Kääb, A., Wagner, S., 2004. Characteristics and potential climatic significance of “miniature ice caps” (crest-and cornice-type low-altitude ice archives). *Journal of Glaciology* 50, 129–136.
- Heim, A., 1932. Bergsturz und Menschenleben. *Beiblatt zur Vierteljahresschrift der Naturforschenden Gesellschaft in Zürich* 20, 217.
- Hoelzle, M., 1994. Permafrost und Gletscher im Oberengadin. Grundlagen und Anwendungsbeispiele für automatisierte Schätzverfahren. *Mitteilungen der VAW-ETH Zürich*, vol. 132, 119 pp.
- Hoelzle, M., 1996. Mapping and modelling of mountain permafrost distribution in the Alps. *Norwegian Journal of Geography* 50, 11–15.
- Hoelzle, M., 1998. Rock Glaciers, Upper Engadin, Switzerland. International Permafrost Association, Data and Information Working Group, NSIDC. University of Colorado at Boulder. CD-ROM.
- Hoffmann, T., Schrott, L., 2002. Modelling sediment thickness and rockwall retreat in an Alpine valley using 2D-seismic refraction (Reintal, Bavarian Alps). *Zeitschrift für Geomorphologie* 127, 153–173.
- Hoffmann, T., Schrott, L., 2003. Determining sediment thickness of talus slopes and valley fill deposits using seismic refraction — a comparison of 2D interpretation tools. *Zeitschrift für Geomorphologie* 132, 71–87.
- Holzhauser, H., 1995. Gletscherschwankungen innerhalb der letzten 3200 Jahre am Beispiel des Grossen Aletsch- und des Gornergletschers. Neue Ergebnisse. In: Salm, B. (Ed.), *Gletscher im ständigen Wandel. vdf-Hochschulverlag AG an der ETH, Zürich*, pp. 101–122.
- Hübl, J., Kienholz, H., Loipersberger, A. (Eds.), 2002. DOMODIS — Documentation of Mountain Disasters. State of Discussion in the European Mountain Areas. International Research Society INTERPRAEVENT. Series 1, Manual 1, Klagenfurt (Austria). 40 pp.
- Hurni, L., 1995. Digital cartographic and topographic products from the Swiss Federal Office of Topography. *LIBER Quarterly. The Journal of European Research Libraries* 5, 255–261.
- Imhof, M., 1996. Modelling and verification of the permafrost distribution in the Bernese Alps (Western Switzerland). *Permafrost and Periglacial Processes* 7, 267–280.
- Joerin, U., Schlüchter, C., 2005. Centennial Scale Holocene Alpine Glacier Fluctuations. EGU, General Assembly, Vienna: Geophysical Research Abstracts, vol. 7. EGU-A-08540, CD-ROM.
- Kääb, A., 2005. Remote sensing of mountain glaciers and permafrost creep. *Physische Geographie*, vol. 48. Zurich. ISBN 3 85543 244 9. 264 pp.
- Kääb, A., Vollmer, M., 2000. Surface geometry, thickness changes and flow fields on permafrost streams: automatic extraction by digital image analysis. *Permafrost and Periglacial Processes* 11 (4), 315–326.
- Karssen, D., 2002. Building dynamic spatial environmental models. *Netherlands Geographical Studies*, vol. 305. University of Utrecht. 222 pp.
- Kieffer, H.H., et al., 2000. New eyes in the sky measure glaciers and ice sheets. EOS, Transactions American Geophysical Union 81 (265), 270–271.
- Kneisel, C., Hauck, C., Vonder Mühll, D., 2000. Permafrost below the timberline confirmed and characterized by geoelectrical resistivity measurements, Bever Valley, Eastern Swiss Alps. *Permafrost and Periglacial Processes* 11, 295–304.
- Konrad, S.K., Humphrey, N.F., 2000. Steady-state flow model of debris-covered glaciers (rock glaciers). *Proceedings of the Workshop on 'Debris-covered Glaciers'. IAHS Publ., Seattle, Washington, USA*, pp. 255–263.
- Konrad, S.K., Humphrey, N.F., Steig, E.J., Clark, D.H., Potter Jr., N., Pfeffer, W.T., 1999. Rock glacier dynamics and paleoclimatic implications. *Geology* 27, 1131–1134.
- Labeyrie, L., Cole, J., Alverson, K.D., Stocker, T., 2003. The history of climate dynamics in the Late Quaternary. In: Alverson, K.D., Bradley, R.S., Pedersen, T.F. (Eds.), *Paleoclimate, Global Change and the Future*. Springer, Berlin, Heidelberg, pp. 33–61.

- Laustela, M., Egli, M., Frauenfelder, R., Kääb, A., Maisch, M., Haeberli, W., 2003. Weathering rind measurements and relative age dating of rockglacier surfaces in crystalline regions of the Eastern Swiss Alps. In: Phillips, M., Springman, S., Arenson, L. (Eds.), 8th International Conference on Permafrost, Proceedings. Swets and Zeitlinger, Lisse, Zürich, pp. 627–632.
- Leyssinger Vieli, G.J.-M.C., 2004. Modeling advance and retreat of alpine and rock glaciers. *Mitteilungen der VAW-ETH Zürich*, vol. 185. 102 pp.
- Lundell, M., 1996. Qualitative modelling and simulation of spatially distributed parameter systems. PhD Thesis, EPFL-Swiss Federal Institute of Technology, Lausanne. 264 pp.
- Maisch, M., 1992. Die Gletscher Graubündens: Rekonstruktionen und Auswertung der Gletscher und deren Veränderungen seit dem Hochstand von 1850 im Gebiet der östlichen Schweizer Alpen (Bündnerland und angrenzende Regionen). *Physische Geographie*, vol. 33A/B. Zürich. 324/128 pp.
- Maisch, M., Wipf, A., Denneler, B., Battaglia, J., Benz, C., 2000. Die Gletscher der Schweizer Alpen. Gletscherhochstand 1850, Aktuelle Vergletscherung, Gletscherschwund-Szenarien. Schlussbericht NFP, vol. 31. vdf-Hochschulverlag ETH, Zürich. 373 pp.
- Matsuoka, N., 1990. The rate of rock weathering by frost action: field measurements and predictive model. *Earth Surface Processes and Landforms* 15, 73–90.
- Matsuoka, N., Ikeda, A., 2001. Geological control on the distribution and characteristics of talus-derived rock glaciers. *Annual Report of the Institute of Geoscience, University of Tsukuba*, vol. 27, pp. 11–16.
- Moore, I.D., Grayson, R.B., Ladson, A.R., 1990. Digital terrain modelling: a review of hydrological, geomorphological and biological applications. *Hydrological Processes* 5, 3–30.
- Olyphant, G.A., 1983. Computer simulation of rock-glacier development under viscous and pseudoplastic flow. *Geological Society of America Bulletin* 94, 499–505.
- Olyphant, G.A., 1987. Rock glacier response to abrupt changes in talus production. In: Giardino, J.R., Shroder, J.F., Vitek, J.D. (Eds.), *Rock Glaciers*. Allen and Unwin, London, pp. 55–64.
- Paterson, W.S.B., 1994. *The Physics of Glaciers*, 3rd edition. Pergamon Press Ltd., London. 380 pp.
- Paul, F., 2003. The new Swiss Glacier Inventory 2000. Application of Remote Sensing and GIS. PhD Thesis, University of Zurich. 192 pp.
- Poser, H., 1954. Die Periglazial-Erscheinungen in der Umgebung der Gletscher des Zemmgrundes (Zillertaler Alpen). *Göttinger Geographische Abhandlungen* 15, 125–180.
- Prick, A., 2003. Frost weathering and rock fall in an arctic environment, Longyearbyen, Svalbard. In: Phillips, M., Springman, S., Arenson, L. (Eds.), 8th International Conference on Permafrost, Proceedings. Swets and Zeitlinger, Lisse, Zurich, pp. 907–912.
- Rapp, A., 1960. Recent development of mountain slopes in Kärkevagge and surroundings, northern Scandinavia. *Geografiska Annaler* 42, 71–200.
- Roberts, N., 2000. *The Holocene. An Environmental History*. Blackwell Publishers Ltd, Oxford. 316 pp.
- Roer, I., Kääb, A., Dikau, R., 2005. Rockglacier kinematics derived from small-scale aerial photography and digital airborne pushbroom imagery. *Zeitschrift für Geomorphologie*. N.F. 49 (1), 73–87.
- Schwarb, M., Frei, C., Schär, C., Daly, C., 2000. Mean Annual Precipitation throughout the European Alps 1971–1990. *Hydrological Atlas of Switzerland*, Zurich.
- Sipper, M., 1997. *Evolution of parallel cellular machines: the cellular programming approach*, XIII. Springer-Verlag, Heidelberg. 198 pp.
- Skaug, Ø., 2000. Påvirkning fra skala, datastruktur og representasjon på kvalitet av terrengparametre brukt i digital relieffanalyse. Unpublished MSc-thesis, Department of Physical Geography, University of Oslo. 88 pp.
- Stocker-Mittaz, C., Hoelzle, M., Haeberli, W., 2002. Permafrost distribution modeling based on energy-balance data: a first step. *Permafrost and Periglacial Processes* 13 (4), 271–282.
- Taschner, S., Ranzi, R., 2002. Landsat-TM and ASTER data for monitoring a debris covered glacier in the Italian Alps within the GLIMS project, IGARSS 2002. *Proceedings, Toronto, Canada*, pp. 1044–1046.
- Van Deursen, W.P.A., 1995. *Geographical Information Systems and Dynamic Models — Development and application of a prototype spatial modelling language*. PhD Thesis, University of Utrecht. 126 pp.
- Van Dijke, J.J., van Westen, C.J., 1990. Rockfall hazard, a geomorphological application of neighbourhood analysis with ILWIS. *ITC Journal* 1, 40–44.
- VAW, 1992a. Murgänge 1987: Dokumentation und Analyse. Teil 1. Bericht im Auftrag des Bundesamtes für Wasserwirtschaft. 97.6, Versuchsanstalt für Wasserbau, Hydrologie und Glaziologie. ETH, Zurich.
- VAW, 1992b. Murgänge 1987: Dokumentation und Analyse. Teil 2. Bericht im Auftrag des Bundesamtes für Wasserwirtschaft. 97.6, Versuchsanstalt für Wasserbau, Hydrologie und Glaziologie. ETH, Zurich.
- Von Neumann, J., 1966. *Theory of Self-reproducing Automata*. University of Illinois Press, Urbana. 388 pp.
- Vonder Mühll, D., 1993. Geophysikalische Untersuchungen im Permafrost des Oberengadins, vol. 122. *Mitteilungen der VAW-ETH, Zürich*. 222 pp.
- Vonder Mühll, D., Holub, P., 1992. Borehole logging in Alpine permafrost, Upper Engadin, Swiss Alps. *Permafrost and Periglacial Processes* 3, 125–132.
- Vonder Mühll, D., Arenson, L., Springman, S., 2001. Two new boreholes through the Murtèl–Corvatsch rock glacier, Upper Engadin, Switzerland. In: Rea, B. (Ed.), 1st European Permafrost Conference, Rome, p. 83.
- Wagner, S., 1992. Creep of Alpine permafrost, investigated on the Murtèl rock glacier. *Permafrost and Periglacial Processes* 3, 157–162.
- Wagner, S., 1996. Dreidimensionale Modellierung zweier Gletscher und Deformationsanalyse von eisreichem Permafrost. *Mitteilungen der VAW-ETH Zürich*, vol. 146. 104 pp.
- Wesseling, C.G., Karssenbergh, D., Van Deursen, W.P.A., Burrough, P.A., 1996. Integrating dynamic environmental models in GIS: the development of a Dynamic Modelling language. *Transactions in GIS* 1, 40–48.
- Whalley, W.B., Martin, H.E., 1992. Rock glaciers. Part II: Models and mechanisms. *Progress in Physical Geography* 16, 127–186.
- Websites:
- Brändli, M., 2001. Steinschlagmodellierung. [http://www.geo.unizh.ch/gis/teaching/courses/gis2/infos/schlussberichte00\\_01/gr12/vorgehen.html](http://www.geo.unizh.ch/gis/teaching/courses/gis2/infos/schlussberichte00_01/gr12/vorgehen.html) (access date: 22.05.2007).